# Analysis of surface preparation treatments for coating tungsten carbide substrates with diamond thin films

S. CHATTERJEE, A. G. EDWARDS*, A. NICHOLS*, C. S. FEIGERLE*
*Department of Industrial Engineering and *Department of Chemistry, The University of Tennessee, Knoxville, TN 37996, USA*

The effect of various substrate surface treatments on (i) the pre-growth topography and composition of the treated substrate, and (ii) the quality of diamond thin films produced by hot-filament chemical vapour deposition on tungsten carbide substrates, is reported. Two different substrate grain sizes were subjected to various surface treatments. They were then examined for surface material composition and topography using scanning electron microscopy and X-ray diffraction (XRD). Subsequently, diamond films were deposited on the samples and their quality analysed by Raman spectroscopy and XRD techniques. These analyses do not indicate a strong dependence between the substrate grain size and film quality. However, the surface-treatment method affects the resulting substrate surface topography and film quality.

## 1. Introduction

Diamond thin films, due to the unique properties of diamond, hold significant promise as the material of choice for many diverse applications, such as, semiconductors, optics, acoustics, and as coatings for metal cutting tools [1–4]. With the development of low-pressure techniques for depositing diamond films, the production and application of these films have increased. When applied as coatings for metal cutting tools, the high hardness, low coefficient of friction, chemical inertness, and refractoriness of diamond can be effectively utilized to improve tool life.

The use of diamond thin films as a coating for metal cutting tools is still in the developmental stages. While diamond-coated tungsten carbide (WC) or silicon nitride ($Si_3N_4$) inserts are currently commercially available [5], effective coating of non-flat surfaces, such as cylinders, drills, end mills, taps, etc., is a challenge because of film adhesion problems associated with the complex substrate geometries. This is more pronounced with WC than $Si_3N_4$ because of large differences in the thermal expansion coefficient of WC and diamond. Thus, many cutting tool manufacturers have migrated toward using $Si_3N_4$ as substrate material. However, next to high-speed steel, WC is probably the most widely used cutting tool material [6]. Therefore, it is important that the adhesion aspects of WC–diamond composite be studied for improvement.

Substrate surface preparation is usually the first step in any thin-film deposition process and governs film adhesion to the substrate. This is evident in reported results for various ceramic films [7–10]. In the present study, the effects of various surface treatments on pre-deposition topography and composition, as well as on the quality and morphology of the deposited films, have been investigated. The effects of varying grain sizes were also studied and compared for substrates with the same binder concentration. Studies on film adhesion, stresses, and performance will be presented in a separate publication.

## 2. Review of previous research

Effective substrate surface treatment is essential for depositing quality diamond films. These treatments alter the surface topography and aid in film nucleation and growth. For example, growth on silicon wafers is usually preceded by scratching the substrate with diamond powder in a solvent such as ethanol, or with diamond paste [11–13].

The surface preparation of WC for diamond growth is more complex due to the presence of cobalt which inhibits diamond nucleation and subsequent film growth by forming complex carbides. Thus, cobalt must be removed before growth [14–15]. However, this removal must be restricted to the surface only, otherwise the effectiveness of cobalt as a binder to the WC matrix is lost, resulting in a rapid loss of tool material strength under application conditions.

Saijo *et al.* [15] and Takatsu *et al.* [16] have shown that decarburizing WC substrate prior to plasma deposition results in higher indentation adhesion. However, their samples contained 99.5% WC and no cobalt. The decarburization was performed by microwave plasma and subsequently, the samples were scratched by diamond powder. The decarburized substrate was observed by X-ray diffraction (XRD) to contain only tungsten which produced fine-grained

0022–2461  

WC after diamond growth. This grain size was finer than the non-decarburized WC substrate. The authors attributed the improved adhesion performance to the generation of many fine grains of WC and increased surface contact area at the film–substrate interface. The lack of cobalt in the WC in both studies restricts the utility of this study to cobalt-bearing substrates and raises the question of decarburizing effects in the presence of cobalt. Kuo *et al.* [17] reported improved adhesion of microwave plasma-deposited diamond-coated WC (94.3% WC–5.7% Co) substrates. The surface treatment consisted of scratching with 20–40 μm diamond powder and polishing with a 1 μm diamond paste. The authors observed a wave-like morphology of the film for non-treated substrates. The existence of this morphology was attributed to the existence of large voids at the interface. For the treated substrates, a denser morphology without voids was observed. This resulted in better adhesion and was ascribed to a higher nucleation density. The authors do not mention cobalt removal as part of the surface treatment in their study.

Cobalt removal by acid etching is another surface treatment process. Huang *et al.* [18] treated cobalt-containing WC substrates with a 1:3 vol/vol solution of $HNO_3$ and $H_2O$ and then polished them using a 6 μm diamond suspension in water prior to hot-filament chemical vapour deposition (HFCVD) of diamond. Their study did not examine the post-treatment nature of the substrate surface or the effect of various treatments on film growth.

Tsai *et al.* [19] reported the use of an $HNO_3$ and $CH_3COOH$ solution for cobalt removal. Post-etching microscopy of the substrates revealed voids between WC grains and spontaneous peeling of film upon cooling.

The above literature survey indicates that while various surface treatments have been used for substrate preparation, a comprehensive comparison of the treatment effects is lacking. A structured analysis and comparison of the effects of various treatments on the pre-deposition surface topography and composition and post-deposition film quality and composition, particularly for WC substrates, is needed. Based on the literature survey, the effectiveness of acid etching of WC for improving film quality warrants further investigation.

This study, therefore, focused on investigating the effect of various treatments on the pre-deposition surface topography and composition and post-deposition film quality and composition.

## 3. Experimental procedure

### 3.1. Specimen details and preparation

Table I provides specifications for the two types of samples used in the study.

All samples were cylindrical rods, 0.25 in. (~0.64 cm) diameter and 0.5 in. (~1.27 cm) long. The rods were ground using a 220 grit diamond wheel, polished and ultrasonically cleaned in reagent-grade acetone to remove surface organics. Three different preparation methods were used. In the first method, the sample was only ultrasonically cleaned with acetone and served as a control sample. In the second method, an acetone-treated sample was ultrasonically treated with a 1:1 vol/vol $HNO_3 + H_2O$ mixture for 15 min, rinsed with 18 Ω water and sonicated again for 5 min in 18 Ω water. The third treatment was a proprietary chemical treatment for surface cobalt removal [20]. Three samples treated by the third method were studied. Half of one of these two samples was scratched with diamond paste followed by ultrasonic cleaning in acetone & then methanol.

### 3.2. Scanning electron microscopy (SEM) examination conditions

The samples were analysed using a Hitachi S 800 SEM prior to diamond deposition. The instrument is equipped with an electron gun with voltage maintained at 19 kV for all analyses. The samples were loaded individually and examined by : (i) the secondary electron (SE) detector, (ii) the backscattered electron (BSE) detector, (iii) the X-ray scintillation (XRS) detector. A 100 keV filament-to-target potential was maintained for the X-ray spectra with a 158.00 eV detector resolution and 76.00 take-off angle.

### 3.3. Film deposition

Diamond films were deposited using HFCVD in a reactor constructed from a high-vacuum six-way cross. Growth was performed with a 1% methane/hydrogen gaseous mixture at a 100 standard $cm^3\ min^{-1}$ flow rate, 38–40 torr (1 torr = 133.322 Pa) chamber pressure, and substrate and filament temperatures of 1050 and 2120 K, respectively. Filament and substrate brightness temperatures were measured with a disappearing filament-type optical pyrometer and are reported without further correction for emissivity.

### 3.4 Raman spectroscopy

The diamond films were analysed using a Dilor *XY* Raman spectrometer with a microscope attachment and CCD detector. Spectra were recorded using 100 mW of 514.5 nm excitation focused on the samples through a $\times 80$ or $\times 100$ objective of the microscope. No degradation of the samples was observed under these conditions. The Raman shifts reported in this paper are based upon calibrating the instrument using the 1332 $cm^{-1}$ line from a single-crystal diamond sample.

### 3.5. XRD conditions

The films were subjected to XRD and the [1 0 2] WC plane was step-scanned using a chromium radiation of

TABLE I Sample specifications

| Sample | Composition | Grain size (μm) |
|---|---|---|
| A | 94% WC, 6% Co | 0.8–1.0 |
| B | 94% WC, 6% Co | 1.7 |

0.228 97 nm wavelength. A rectangular collimator of 5 mm aperture was used during scanning. The 2θ diffraction values were utilized to determine the presence of various components.

## 4. Results and discussion

The samples were analysed before and after diamond film deposition to investigate various treatment effects on surface topography, composition, and ultimately, film growth. The results of post-treatment surface topography and composition analysis are discussed first, and analysis of the quality of the diamond films and film–substrate interface composition follows.

### 4.1. Post-treatment surface topography analysis

The treatment effects on surface topography and composition prior to diamond deposition were investigated. The SE and BSE detectors in SEM provide different information. The SE detector enables good depth-of-field images and shows detailed surface topography. The brightness of images acquired with a BSE detector correlates with the atomic number of the material probed. Under identical instrumental conditions, brighter areas are observed for higher atomic number species [21].

Fig. 1 shows an SEM image obtained with the SE detector of a type B sample treated with acetone only, to remove organic contaminants. The surface appears fairly uneven and the observed striations are the marks from the grinding process. Fig. 2 shows the same image for sample B with nitric acid treatment. The examined area here appears to be much flatter in comparison to the examined area of Fig. 1. Figs 3 and 4 show the respective images obtained with the BSE detector. A comparison of the two images indicates more contrast in surface brightness in Fig. 4 than in Fig. 3. This implies that the composition of the surface has been altered by the nitric acid treatment. The change in brightness suggests the removal of lighter atomic number species by nitric acid [21].

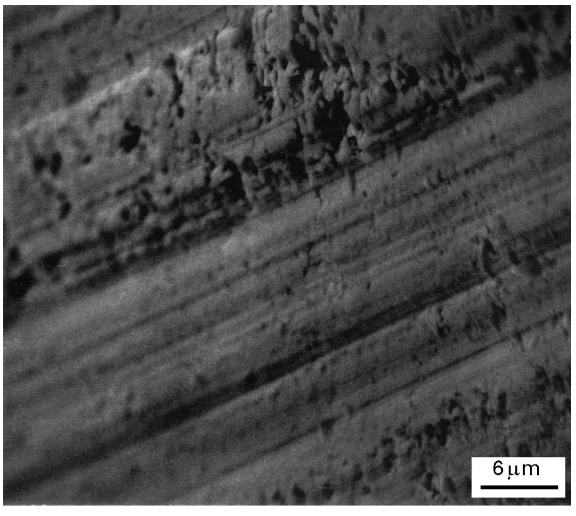


*Figure 1* SE detector image of sample B; acetone treatment.

Figs 5 and 6 show the SE and BSE detector images for a type B sample treated by the proprietary process. The micrograph Fig. 5 clearly demonstrates a rougher topography and surface porosity than is obtained by

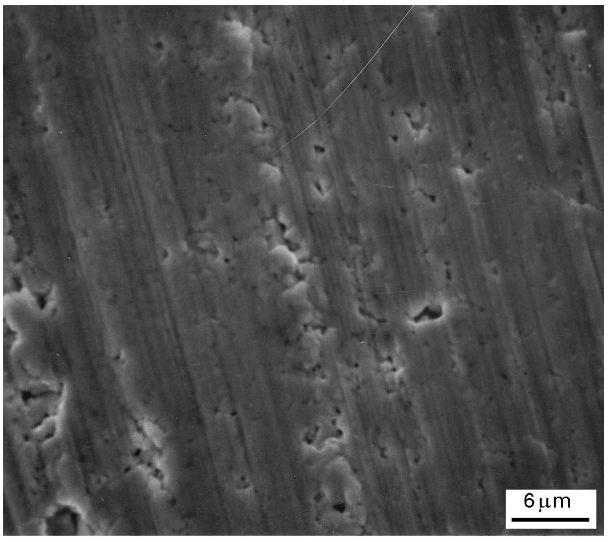


*Figure 2* SE detector image of sample B; $HNO_3$ treatment.

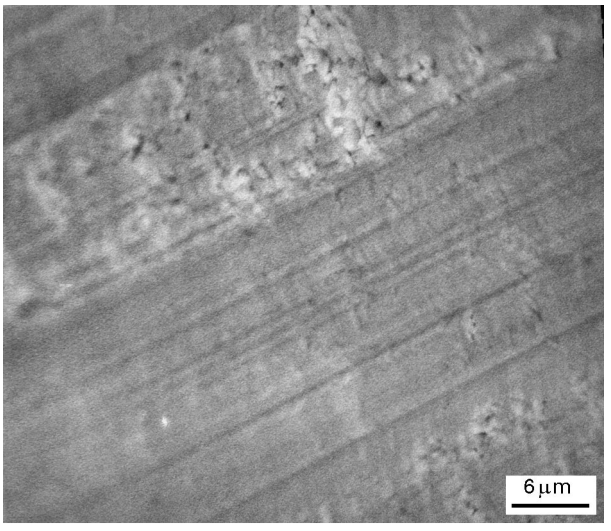


*Figure 3* BSE detector image of sample B; acetone treatment.

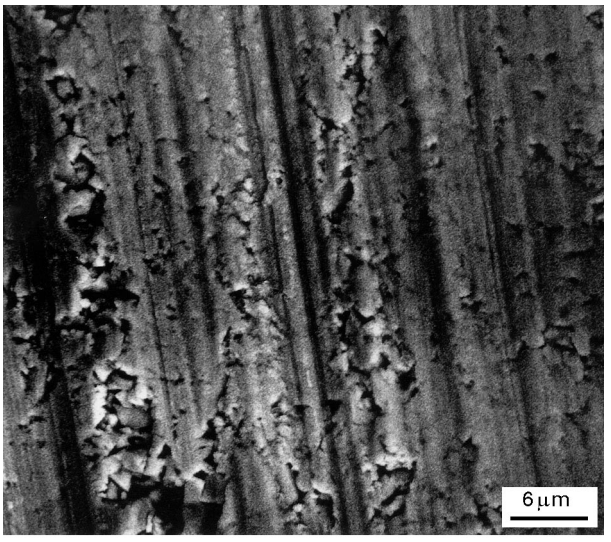


*Figure 4* BSE detector image of sample B; $HNO_3$ treatment.

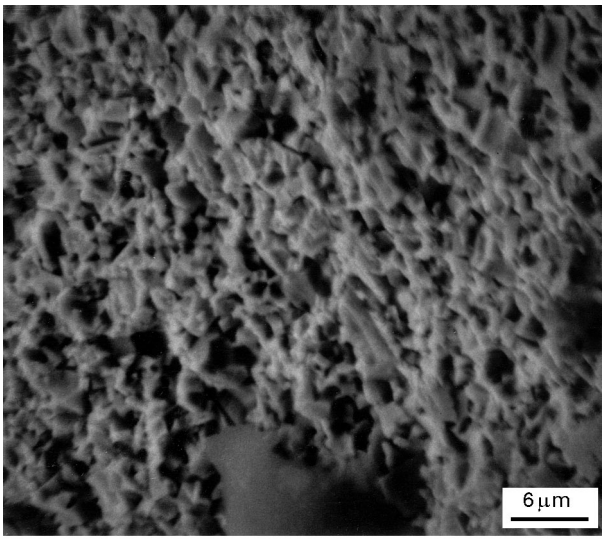


*Figure 5* SE detector image of sample B with proprietary treatment.

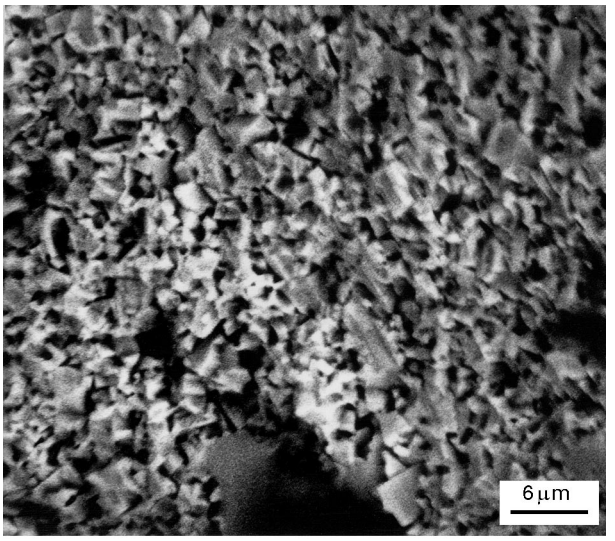


*Figure 6* BSE detector image of sample B with proprietary treatment.

the nitric acid treatment. It is evident that the proprietary treatment changes the nature of the WC surface much more than does nitric acid. A comparison of the BSE images, Figs 4 and 6, indicates higher brightness in Fig. 6, suggesting the presence of average higher atomic number species on the surface examined. Furthermore, this brightness appears to be uniformly spaced throughout the surface indicating a uniformly rougher surface. This would support the contention that the proprietary treatment depletes the surface of lower atomic number species, such as cobalt, and enriches the surface in higher atomic species, such as tungsten. It is interesting to note that the surfaces generated by the proprietary treatment bear similarities to those reported by Saijo *et al.* [15] and Takatsu *et al.* [16] for decarburized WC surfaces without cobalt.

## 4.2. Post-treatment surface composition analysis

The X-ray spectra of all samples were acquired and examined. Figs 7, 8, and 9 show the X-ray spectra of the samples treated with acetone, nitric acid and proprietary treatment respectively. The peaks between 8.0 and 12.0 keV are for $L_\alpha$, $L_\beta$, and $L_\gamma$ bands for tungsten. In Fig. 7, three fairly intense peaks are seen between 6.0 and 8.0 keV. The intense peak at 6.4 keV corresponds to the $K_\alpha$ line for iron and is believed to be due to contaminants from the grinding process. The two higher energy bands correspond to the $K_\alpha$ and $K_\beta$ for cobalt, with the lower energy band for cobalt probably overlapping the $K_\beta$ band for iron. If

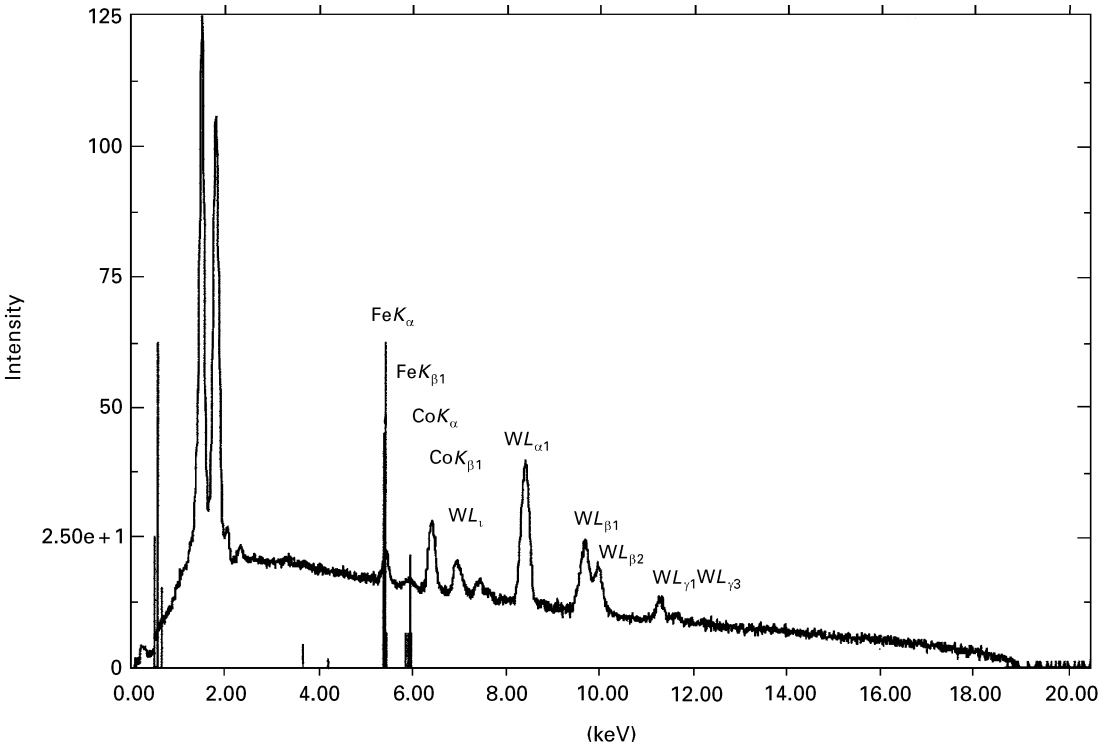


*Figure 7* X-ray spectrum of WC treated with acetone.

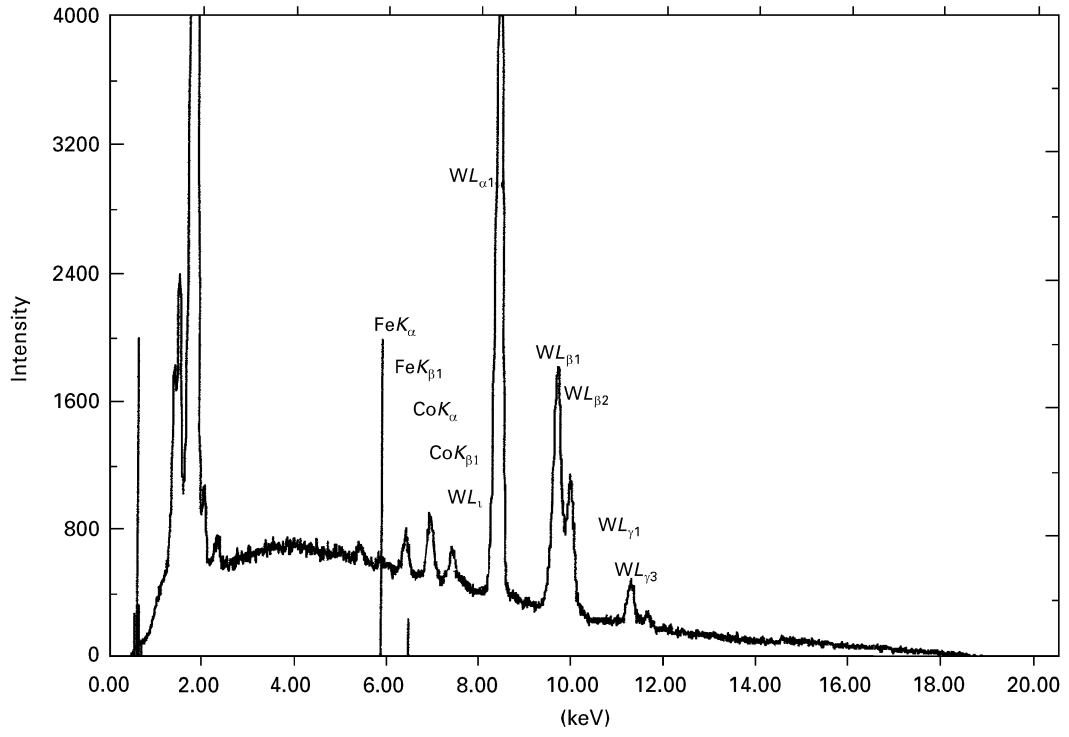


*Figure 8* X-ray spectrum of WC treated with $HNO_3$/acetone/methanol.

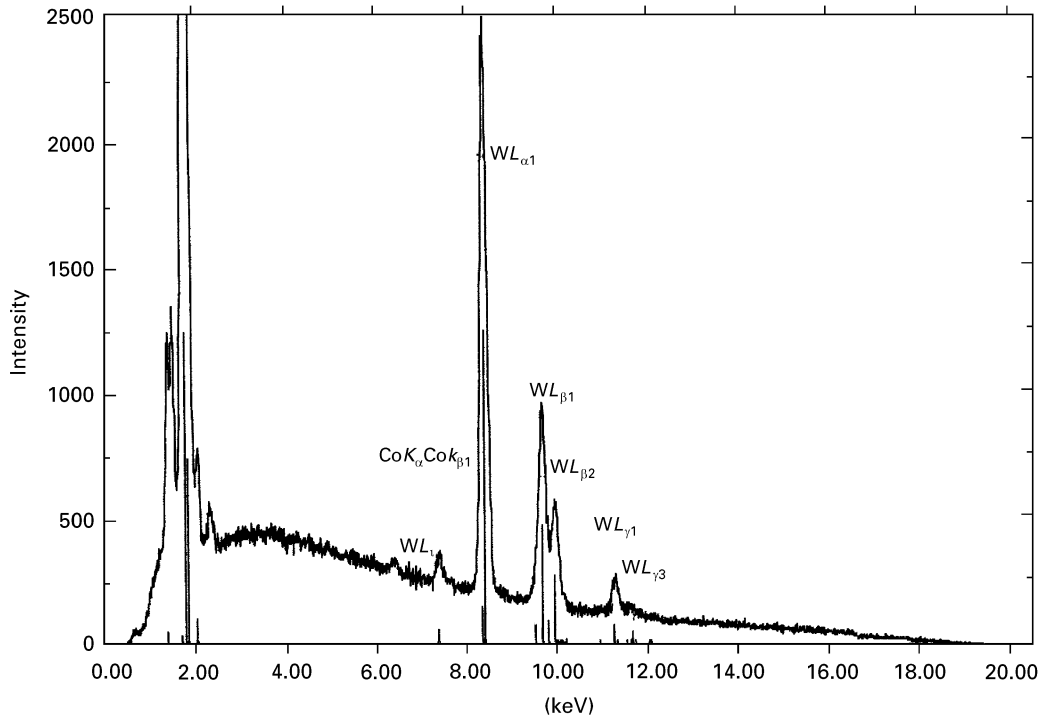


*Figure 9* X-ray spectrum of WC treated with proprietary treatment.

a comparison of the relative intensities of the peaks between 6–8 keV and 8–12 keV is taken as a measure of the relative concentrations of non-W to W metals, Figs 8 and 9 indicate that both the nitric acid and proprietary treatments removed non-tungsten metals. The proprietary treatment was more effective in removing cobalt than nitric acid etching.

## 4.3. XRD analysis

X-ray diffraction was performed on the treated type A samples using the XRD conditions described earlier. The 2θ diffraction angles determined for each sample indicate the presence or absence of particular species. Table II shows the 2θ angles and the species detected for type A samples which have been treated by the proprietary (PT), nitric acid (NA), and acetone (AT)

TABLE II Diffraction angles and species present

| | Treatment Type | | |
|---|---|---|---|
| | PT | NA | AT |
| Diffraction angle, 2θ (deg) | 135.5 (WC)<br>124.39 (W) | 135.5 (WC)<br>131.5 (Co) | 135.5 (WC)<br>131.5 (Co) |

TABLE III Summary of treatment effects

| Treatment | Detection method | | |
|---|---|---|---|
| | SE | BSE | XRD |
| AT | U | U | WC, Co |
| NA | U | U | WC, Co |
| PT | URP | URP | WC, W |

treatments. The species present, W, WC, and Co, are indicated within parentheses. It is evident that the acetone and nitric acid treatments are unable completely to remove cobalt from the surface. This finding is in contrast to some reports, (for example [18, 19]), which claim complete cobalt removal by nitric acid treatment. These reports, however, do not present surface analysis results for the treated surfaces.

The results of the surface treatment processes for the type A and B samples are summarized in Table III. In this table, U and URP represent uneven, uniform, and uneven, rough and porous, respectively, and refer, qualitatively, to the SEM surface topography discussed earlier. The species present, as determined by XRD analysis, are also indicated.

## 4.4. Diamond film quality analysis

The effects of the surface treatments on the resulting diamond film quality and the presence of species in the film are presented and discussed. Table IV summarizes the Raman intensities, shifts, full-width at half maximum (FWHM), and diamond-to-graphite intensity ratios for type A and B samples subjected to the various treatments. The values in this table are the averages of three readings for each sample treatment. The treatments are as indicated earlier. In addition, "scratch" refers to scratching half of a sample with diamond paste (see Section 3.1).

Table IV exhibits intensity level and ratio variations between variously treated samples. It is also evident from the FWHM and intensity values that follow-up scratching (paste treatment) degrades the film. This is in agreement with the SEM observations from Fig. 5. It is possible that once cobalt removal and sufficient surface porosity is obtained, additional surface degradation by scratching actually retards growth. This finding is in contrast to those reported in the literature citing enhanced diamond film growth from scratched surfaces due to increased nucleation.

Grain-size effects on film growth and quality do not seem to be conclusive. However, the data show that the PT treatment of type A sample (0.8–1.0 μm grain size) enabled the best film growth with the highest intensities.

TABLE IV Raman shifts and intensities

| Sample type | Treatment | Shift ($cm^{-1}$) | Intensity (Arb. units) | FWHM | Intensity ratio |
|---|---|---|---|---|---|
| A | NA | 1337 | 33188 | 7.5 | 58 |
| A | PT | 1337 | 43841 | 7.2 | 96 |
| A | PT | 1338 | 37265 | 8.3 | 69 |
| | S | 1339 | 33976 | 8.7 | 56 |
| B | PT | 1338 | 31448 | 8.0· | 90 |
| | S | 1338 | 37871 | 7.5 | 82 |

TABLE V Diffraction angles and species present after HFCVD

| | Treatment type | | |
|---|---|---|---|
| | PT/CVD | NA/CVD | AT |
| Diffraction angle, 2θ (deg) | 135.69 (WC)<br>130.9 (D) | 135.69 (WC)<br>130.9 (D) | 135.5 (WC)<br>131.5 (Co) |

Fig. 10a shows a typical Raman shift for the diamond film. A significant Raman shift from the first-order diamond band (at 1332 $cm^{-1}$) is observed in this figure. Shifts in Raman positions indicate the presence of stresses in the film [22, 23]. Positive shifts in Raman positions have been used to indicate the presence of compressive film stresses [22]. The presence of compressive stresses is also evident from the data in Table IV for all the samples and treatments. Compressive film stresses are good from a machining perspective because they may yield better adhesion during machining. Also, the data seem to indicate that a combination of fine-grain WC substrate, complete cobalt removal, and a rough and porous surface (sample A, PT) results in best diamond growth. This is interesting in metal cutting finishing operations, where stronger fine grains (micro-grains) can accommodate higher finishing speeds and lower feeds thereby enabling better finishes [24].

Fig. 10b shows a micrograph for the PT sample. The diamond growth is dense and the observed undulations result from film growth on grinding striations (see Fig. 1).

The results of XRD analysis performed on pretreated (AT, NA, and PT processes), diamond deposited, type A samples, are given in Table V. The WC, Co, and D in the table indicate the presence of tungsten carbide, cobalt, and diamond, respectively. It is clear from the 2θ diffraction data that NA and PT treated samples exhibited the presence of diamond. The last column (AT treatment only) is for comparison and indicates almost no diamond growth on the one sample which showed evidence of surface cobalt.

## 5. Conclusion

In this study, the effects of various treatments on the pre-deposition surface topography and subsequent film quality and composition of HFCVD diamond thin films on WC substrates, have been examined. The results indicate that complete surface cobalt removal and generation of a rough, porous surface is essential

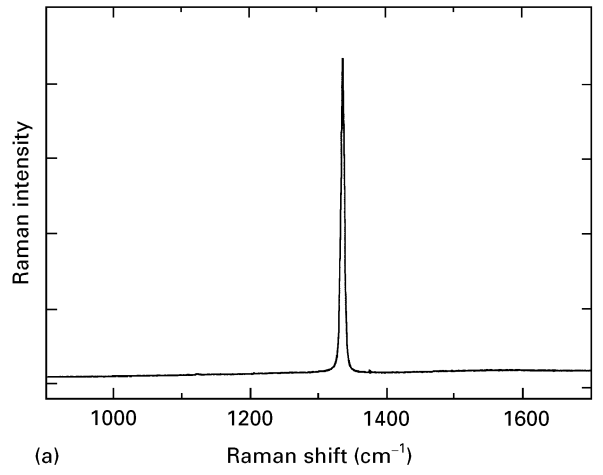


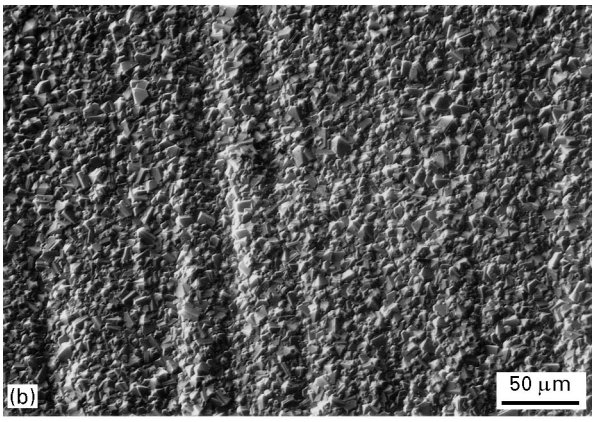


*Figure 10* (a) A typical Raman spectrograph of a diamond film. (b) A scanning electron micrograph of a PT sample.

for quality film growth. It was also found that nitric acid etching may not completely remove cobalt from the surface and this is correlated with a reduction in film quality. The micro-grain-sized substrates were observed to yield superior films. All films showed positive Raman shifts, an indication of the presence of compressive stresses.

## 6. Recommendations for future research

1. Determine the levels of film stresses for WC substrates. This is being investigated and will be reported soon.

2. Determine the dependence of substrate geometry on film stresses.

3. Perform adhesion studies of HFCVD films on WC substrates to investigate the grain size and film-quality dependence.

4. Examine the effect of growth parameters, such as, growth time, substrate temperatures, filament geometry, on the film quality and composition.

5. Based on the above develop appropriate growth and property predictive models.

## Acknowledgements

The authors gratefully acknowledge the financial support provided by the Center for Materials Processing, The University of Tennessee, Knoxville, and by the National Science Foundation (grant CTS-9202575). Sample supply from CARMET Inc., Duncan, SC, and assistance in sample preparation by SP$^3$, Mountain View, CA, is also gratefully acknowledged. The authors thank Isa Conway, Department of Chemical Engineering, for assistance in the growth reactor design, and Dr David Joy, Department of Molecular Biology, The University of Tennessee, Knoxville, for assistance in the microscope measurement.

## References

1. S. SPEAR, *J. Am. Ceram. Soc.* **72** (1989) 171
2. F. MASON, *Am. Machinist* February (1990) 43.
3. P. K. BACHMANN and R. MESSIER, *CEN May* 15 (1989) 24.
4. P. M. STEPHAN, *Am. Ceram. Soc. Bull.* **71** (1992) 1623.
5. E. E. SPROW, *Manuf. Eng.* February (1995) 41.
6. S. CHATTERJEE, S. CHANDRASHEKHAR, and T. S. SUDARSHAN, *J. Mater. Sci.* **27** (1992) 3409.
7. A. MATTHEWS and A. R. LEFKOW, *Thin Solid Films* **126** (1985) 283.
8. J. VOGEL and R. BOLLIER, in "Balzers Bulletin" (Balzers Tool Coating, North Tonawanda, NY, 1989) p. 99.
9. D. M. MATTOX, *Thin Solid Films* **124** (1985) 3.
10. C. C. CHENG, A. ERDEMIR, and G. R. FENSKE, *Surf. Coat. Technol.* **39**/**40** (1989) 365.
11. S. ABRAHAM, C.J. MCHARGUE, R. E. CLAUSING, L. HEATHERLY, and J. D. HUNN, *Diamond Rel. Mater.* **4** (1995) 261.
12. D. E. PEEBLES and L. E. POPE, *J. Mater. Res.* **5** (1990) 2589.
13. S. K. CHOI, D. Y. JUNG, and H. M. CHOI, *J. Vac. Sci. Technol. A* **14** (1) (1996) 165.
14. S. HOSOMI and I. YOSIDA, "Application of Diamond Films and Related Materials" (Elsevier Science, 1991).
15. K. SAIJO, M. YAGI, K. SHIBUKI and S. TAKATSU, *Surf. Coat. Technol.* **43**/**44** (1990) 30.
16. S. TAKATSU, K. SAIJO, M. YAGI, and K. SHIBUKI, *Mater. Sci. Eng.* **A140** (1991) 747.
17. C.-T. KUO, T.-Y. YEN, and T.-H. HUANG, *J. Mater. Res.* **5** (1990) 2515.
18. T.-H. HUANG, C. T. KUO and T. S. LIN, *Surf. Coat. Technol.* **56** (1993) 105.
19. C. TSAI, J. C. NELSON, W. W. GERBERICH, H. HEBERLEIN, and E. PFENDER, *Diamond Rel. Mater.* **2** (1993) 617.
20. SP$^3$ Inc. Mountain View, CA.
21. J. I. GOLDSTEIN and H. YAKOWITZ, "Practical Scanning Electron Microscopy" (Plenum Press, New York, 1975) p. 107.
22. D. S. KNIGHT and W. B. WHITE, *J. Mater. Res.* **4** (2) (1989) 385.
23. M. HANFLAND, K. SYASSEN, S. FAHY, S. G. LOUIE and M. L. COHEN, *Physics* **139, 140B** (1986) 516.
24. F. MASON, *Manuf. Eng.* January (1995) 27.

*Received 23 August*
*and accepted 30 October 1996*